# Measurement of the B+ and B0 meson lifetimes. — **Source link** ⧉

F. Abe, M. G. Albrow, D. Amidei, C. Anway-Wiese ...+371 more authors

**Institutions:** Yale University

Related papers:

- Measurement of absolute branching fractions of inclusive semileptonic decays of charm and charmed-strange mesons

- Measuring B(D+ → μ+ ν) and the pseudoscalar decay constant fD+

- Study of the K + π + π - final state in B + →J/ψK + π + π - and B + →ψ ' K + π + π -

- Study of the decays B0→D(*)+D(*)-

- Measurement of b quark fragmentation fractions in the production of strange and light B mesons in pp̄ collisions at √s=1.8 TeV
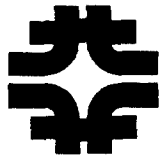
**Fermi National Accelerator Laboratory**

# Measurement of the $B^+$ and $B^0$ Meson Lifetimes

F. Abe et al
The CDF Collaboration

*Fermi National Accelerator Laboratory*
*P.O. Box 500, Batavia, Illinois 60510*

January 1994

## Disclaimer

# Measurement of the $B^+$ and $B^0$ Meson Lifetimes

F. Abe,[13] M. Albrow,[7] D. Amidei,[16] C. Anway-Wiese,[4] G. Apollinari,[26] H. Areti,[7] P. Auchincloss,[25] F. Azfar,[21]

P. Azzi,[20] N. Bacchetta,[18] W. Badgett,[16] M. W. Bailey,[24] J. Bao,[33] P. de Barbaro,[25] A. Barbaro-Galtieri,[14]

V. E. Barnes,[24] B. A. Barnett,[12] P. Bartalini,[23] G. Bauer,[15] T. Baumann,[9] F. Bedeschi,[23] S. Behrends,[2] S. Belforte,[23]

G. Bellettini,[23] J. Bellinger,[32] D. Benjamin,[31] J. Benlloch,[15] D. Benton,[21] A. Beretvas,[7] J. P. Berge,[7] A. Bhatti,[26]

K. Biery,[11] M. Binkley,[7] F. Bird,[28] D. Bisello,[20] R. E. Blair,[1] C. Blocker,[28] A. Bodek,[25] V. Bolognesi,[23] D. Bortoletto,[24]

C. Boswell,[12] T. Boulos,[14] G. Brandenburg,[9] E. Buckley-Geer,[7] H. S. Budd,[25] K. Burkett,[16] G. Busetto,[20]

A. Byon-Wagner,[7] K. L. Byrum,[1] C. Campagnari,[7] M. Campbell,[16] A. Caner,[7] W. Carithers,[14] D. Carlsmith,[32]

A. Castro,[20] Y. Cen,[21] F. Cervelli,[23] J. Chapman,[16] G. Chiarelli,[8] T. Chikamatsu,[30] S. Cihangir,[7] A. G. Clark,[23]

M. Cobal,[23] M. Contreras,[5] J. Cooper,[7] M. Cordelli,[8] D. P. Coupal,[28] D. Crane,[7] J. D. Cunningham,[2] T. Daniels,[15]

F. DeJongh,[7] S. Dell'Agnello,[23] M. Dell'Orso,[23] L. Demortier,[26] B. Denby,[7] M. Deninno,[3] P. F. Derwent,[16] T. Devlin,[27]

M. Dickson,[25] S. Donati,[23] J. P. Done,[29] R. B. Drucker,[14] A. Dunn,[16] K. Einsweiler,[14] J. E. Elias,[7] R. Ely,[14] E. Engels, Jr.,[22] S. Eno,[5] D. Errede,[10] S. Errede,[10] A. Etchegoyen,[7a] Q. Fan,[25] B. Farhat,[15] I. Fiori,[3] B. Flaugher,[7]

G. W. Foster,[7] M. Franklin,[9] M. Frautschi,[18] J. Freeman,[7] J. Friedman,[15] H. Frisch,[5] A. Fry,[28] T. A. Fuess,[28]

Y. Fukui,[13] S. Funaki,[30] G. Gagliardi,[23] M. Gallinaro,[20] A. F. Garfinkel,[24] S. Geer,[7] D. W. Gerdes,[16] P. Giannetti,[23]

N. Giokaris,[26] P. Giromini,[8] L. Gladney,[21] D. Glenzinski,[12] M. Gold,[18] J. Gonzalez,[21] A. Gordon,[9] A. T. Goshaw,[6]

K. Goulianos,[26] H. Grassmann,[28] A. Grewal,[21] G. Grieco,[23] L. Groer,[27] C. Grosso-Pilcher,[5] C. Haber,[14] S. R. Hahn,[7]

R. Hamilton,[9] R. Handler,[32] R. M. Hans,[33] K. Hara,[30] B. Harral,[21] R. M. Harris,[7] S. A. Hauger,[6] J. Hauser,[4]

C. Hawk,[27] J. Heinrich,[21] D. Hennessy,[6] R. Hollebeek,[21] L. Holloway,[10] A. Hölscher,[11] S. Hong,[16] G. Houk,[21] P. Hu,[22]

B. T. Huffman,[22] R. Hughes,[25] P. Hurst,[9] J. Huston,[17] J. Huth,[7] J. Hylen,[7] M. Incagli,[23] J. Incandela,[7] H. Iso,[30]

H. Jensen,[7] C. P. Jessop,[9] U. Joshi,[7] R. W. Kadel,[14] E. Kajfasz,[7] T. Kamon,[29] T. Kaneko,[30] D. A. Kardelis,[10]

H. Kasha,[33] Y. Kato,[19] L. Keeble,[29] R. D. Kennedy,[27] R. Kephart,[7] P. Kesten,[14] D. Kestenbaum,[9] R. M. Keup,[10]

H. Keutelian,[7] F. Keyvan,[4] D. H. Kim,[7] H. S. Kim,[11] S. B. Kim,[16] S. H. Kim,[30] Y. K. Kim,[14] L. Kirsch,[2]

P. Koehn,[25] K. Kondo,[30] J. Konigsberg,[9] S. Kopp,[5] K. Kordas,[11] W. Koska,[7] E. Kovacs,[7a] M. Krasberg,[16] J. Kroll,[7]

M. Kruse,[24] S. E. Kuhlmann,[1] E. Kuns,[27] A. T. Laasanen,[24] S. Lammel,[4] J. I. Lamoureux,[32] T. LeCompte,[10]

S. Leone,[23] J. D. Lewis,[7] P. Limon,[7] M. Lindgren,[4] T. M. Liss,[10] N. Lockyer,[21] O. Long,[21] M. Loreti,[20] E. H. Low,[21]

D. Lucchesi,[23] C. B. Luchini,[10] P. Lukens,[7] P. Maas,[32] K. Maeshima,[7] A. Maghakian,[26] M. Mangano,[23] J. Mansour,[17]

1

M. Mariotti,[23] J. P. Marriner,[7] A. Martin,[10] J. A. J. Matthews,[18] R. Mattingly,[2] P. McIntyre,[29] P. Melese,[26]

A. Menzione,[23] E. Meschi,[23] G. Michail,[9] S. Mikamo,[13] M. Miller,[5] T. Mimashi,[30] S. Miscetti,[8] M. Mishina,[13]

H. Mitsushio,[30] S. Miyashita,[30] Y. Morita,[13] S. Moulding,[26] J. Mueller,[27] A. Mukherjee,[7] T. Muller,[4] P. Musgrave,[11]

L. F. Nakae,[28] I. Nakano,[30] C. Nelson,[7] D. Neuberger,[4] C. Newman-Holmes,[7] L. Nodulman,[1] S. Ogawa,[30] K. E. Ohl,[33]

R. Oishi,[30] T. Okusawa,[19] C. Pagliarone,[23] R. Paoletti,[23] V. Papadimitriou,[7] S. Park,[7] J. Patrick,[7] G. Pauletta,[23]

L. Pescara,[20] M. D. Peters,[14] T. J. Phillips,[6] G. Piacentino,[3] M. Pillai,[25] R. Plunkett,[7] L. Pondrom,[32] N. Produit,[14]

J. Proudfoot,[1] F. Ptohos,[9] G. Punzi,[23] K. Ragan,[11] F. Rimondi,[3] L. Ristori,[23] M. Roach-Bellino,[31] W. J. Robertson,[6]

T. Rodrigo,[7] J. Romano,[5] L. Rosenson,[15] W. K. Sakumoto,[25] D. Saltzberg,[5] A. Sansoni,[8] V. Scarpine,[29] A. Schindler,[14]

P. Schlabach,[9] E. E. Schmidt,[7] M. P. Schmidt,[33] O. Schneider,[14] G. F. Sciacca,[23] A. Scribano,[23] S. Segler,[7] S. Seidel,[18]

Y. Seiya,[30] G. Sganos,[11] M. Shapiro,[14] N. M. Shaw,[24] Q. Shen,[24] P. F. Shepard,[22] M. Shimojima,[30] M. Shochet,[5]

J. Siegrist,[28] A. Sill,[7a] P. Sinervo,[11] P. Singh,[22] J. Skarha,[12] K. Sliwa,[31] D. A. Smith,[23] F. D. Snider,[12] L. Song,[7]

T. Song,[16] J. Spalding,[7] P. Sphicas,[15] A. Spies,[12] L. Stanco,[20] J. Steele,[32] A. Stefanini,[23] K. Strahl,[11] J. Strait,[7]

G. Sullivan,[5] K. Sumorok,[15] R. L. Swartz, Jr.,[10] T. Takahashi,[19] K. Takikawa,[30] F. Tartarelli,[23] Y. Teramoto,[19]

S. Tether,[15] D. Theriot,[7] J. Thomas,[28] R. Thun,[16] M. Timko,[31] P. Tipton,[25] A. Titov,[26] S. Tkaczyk,[7] A. Tollestrup,[7]

J. Tonnison,[24] J. F. de Troconiz,[9] J. Tseng,[12] M. Turcotte,[28] N. Turini,[3] N. Uemura,[30] F. Ukegawa,[21] G. Unal,[21]

S. Vejcik, III,[16] R. Vidal,[7] M. Vondracek,[10] R. G. Wagner,[1] R. L. Wagner,[7] N. Wainer,[7] R. C. Walker,[25] J. Wang,[5]

Q. F. Wang,[26] A. Warburton,[11] G. Watts,[25] T. Watts,[27] R. Webb,[29] C. Wendt,[32] H. Wenzel,[14] W. C. Wester, III,[14]

T. Westhusing,[10] A. B. Wicklund,[1] E. Wicklund,[7] R. Wilkinson,[21] H. H. Williams,[21] P. Wilson,[5] B. L. Winer,[25]

J. Wolinski,[29] D. Y. Wu,[16] X. Wu,[23] J. Wyss,[20] A. Yagil,[7] W. Yao,[14] K. Yasuoka,[30] Y. Ye,[11] G. P. Yeh,[7] M. Yin,[6]

J. Yoh,[7] T. Yoshida,[19] D. Yovanovitch,[7] I. Yu,[33] J. C. Yun,[7] A. Zanetti,[23] F. Zetti,[23] S. Zhang,[15] W. Zhang,[21] and

S. Zucchelli[3]

(CDF Collaboration)

[1] *Argonne National Laboratory, Argonne, Illinois 60439*

[2] *Brandeis University, Waltham, Massachusetts 02254*

[3] *Istituto Nazionale di Fisica Nucleare, University of Bologna, I-40126 Bologna, Italy*

[4] *University of California at Los Angeles, Los Angeles, California 90024*

[5] *University of Chicago, Chicago, Illinois 60637*

[6] *Duke University, Durham, North Carolina 27708*

[7] *Fermi National Accelerator Laboratory, Batavia, Illinois 60510*

[8] *Laboratori Nazionali di Frascati, Istituto Nazionale di Fisica Nucleare, I-00044 Frascati, Italy*

[9] *Harvard University, Cambridge, Massachusetts 02138*

[10] *University of Illinois, Urbana, Illinois 61801*

[11] *Institute of Particle Physics, McGill University, Montreal H3A 2T8, and University of Toronto,*

*Toronto M5S 1A7, Canada*

[12] *The Johns Hopkins University, Baltimore, Maryland 21218*

[13] *National Laboratory for High Energy Physics (KEK), Tsukuba, Ibaraki 305, Japan*

[14] *Lawrence Berkeley Laboratory, Berkeley, California 94720*

[15] *Massachusetts Institute of Technology, Cambridge, Massachusetts 02139*

[16] *University of Michigan, Ann Arbor, Michigan 48109*

[17] *Michigan State University, East Lansing, Michigan 48824*

[18] *University of New Mexico, Albuquerque, New Mexico 87131*

[19] *Osaka City University, Osaka 588, Japan*

[20] *Universita di Padova, Instituto Nazionale di Fisica Nucleare, Sezione di Padova, I-35131 Padova, Italy*

[21] *University of Pennsylvania, Philadelphia, Pennsylvania 19104*

[22] *University of Pittsburgh, Pittsburgh, Pennsylvania 15260*

[23] *Istituto Nazionale di Fisica Nucleare, University and Scuola Normale Superiore of Pisa, I-56100 Pisa, Italy*

[24] *Purdue University, West Lafayette, Indiana 47907*

[25] *University of Rochester, Rochester, New York 14627*

[26] *Rockefeller University, New York, New York 10021*

[27] *Rutgers University, Piscataway, New Jersey 08854*

[28] *Superconducting Super Collider Laboratory, Dallas, Texas 75237*

[29] *Texas A&M University, College Station, Texas 77843*

[30] *University of Tsukuba, Tsukuba, Ibaraki 305, Japan*

[31] *Tufts University, Medford, Massachusetts 02155*

[32] *University of Wisconsin, Madison, Wisconsin 53706*

[33] *Yale University, New Haven, Connecticut 06511*

3

The lifetimes of the $B^+$ and $B^0$ mesons have been measured using fully reconstructed decays. In a sample of $\sim 49600$ $J/\psi \to \mu^+\mu^-$ decays recorded with the Collider Detector at Fermilab, $148 \pm 16$ $B^+$ and $121 \pm 16$ $B^0$ mesons have been reconstructed using the silicon vertex detector. Unbinned likelihood fits to the proper lifetime distributions of these $B$ mesons give $\tau^+ = 1.61 \pm 0.16$ (stat) $\pm$ 0.05 (sys) ps, $\tau^0 = 1.57 \pm 0.18$ (stat) $\pm 0.08$ (sys) ps, and $\tau^+/\tau^0 = 1.02 \pm 0.16$ (stat) $\pm 0.05$ (sys).

PACS numbers: 13.25.+m, 14.40.Jz

Recently, precision measurements of the average $b$-hadron lifetime have been made [1,2]. When combined with a partial decay width and a theoretical model of $B$ decay, such measurements can be used to calculate the Cabibbo-Kobayashi-Maskawa matrix element $|V_{cb}|$ [3]. The simplest $B$ decay model is the spectator model, which predicts equal charged and neutral $B$ meson lifetimes. Although deviations from the spectator model are large in the charm sector, calculations of the $B^+/B^0$ lifetime ratio that include non-spectator diagrams predict $\tau^+/\tau^0$ to be equal to 1.0 within 10-20% [4].

Measurements of $\tau^+$ and $\tau^0$ have been made at PEP and LEP using partially reconstructed decays containing a lepton and a $\overline{D^0}$ or $D^{*-}$ [5]. Indirect measurements have also been made by CLEO and ARGUS, using the ratio of the $B^+$ and $B^0$ semileptonic branching ratios [6]. We present here a measurement of the $\tau^+$ and $\tau^0$ using fully reconstructed decays of the form $B \to \Psi K$, where $\Psi$ represents a $J/\psi$ or $\psi(2S)$ and $K$ represents a $K^+$, $K^*(892)^+$, $K_S^0$, or $K^*(892)^0$ . This is the first high statistics measurement of $B$ meson lifetimes performed using fully reconstructed decays. Throughout this paper, references to a specific charge state imply the charge-conjugate state as well.

The data used in this analysis were collected by the Collider Detector at Fermilab (CDF) during 1992-1993. The data sample corresponds to an integrated luminosity of $\sim 22.4$ pb$^{-1}$ of $p\bar{p}$ collisions at a center-of-mass energy of 1.8 TeV. The CDF detector has been described in detail elsewhere [7]. The main detector systems used for this analysis are the silicon vertex detector (SVX), the central tracking chamber (CTC) and the muon system. The SVX and CTC are located in a 1.4 T solenoidal magnetic field. The SVX consists of 4 layers of silicon strip detectors with $r$-$\phi$ readout, including pulse height information [8]. The pitch between readout strips is 60 $\mu$m (55 $\mu$m) on the 3 inner (1 outer) layers. A spatial resolution of 13 $\mu$m has been obtained. The first measurement plane is located 3 cm from the interaction point, leading to an impact parameter resolution of $(13 + 40/p_T)$ $\mu$m, where $p_T$ is the momentum transverse to the beam direction (measured in GeV/c). The transverse profile of the beam is circular and has an rms

4

of $\sim 40~\mu m$, while the longitudinal beam size is $\sim 30$ cm. The CTC is a cylindrical drift chamber containing 84 layers, which are grouped into alternating axial and stereo superlayers containing 12 and 6 layers respectively. The combined CTC/SVX $p_T$ resolution is $\delta p_T/p_T = [(0.0009 p_T)^2 + (0.0066)^2]^{\frac{1}{2}}$. The central muon system consists of three detector elements. The Central Muon Chambers (CMU), located behind $\sim 5$ interaction lengths $(\lambda_I)$ of material, provide muon identification over 85% of $\phi$ for the pseudorapidity range $|\eta| \leq 0.6$, where $\eta = -\ln[\tan(\theta/2)]$. This $\eta$ region is further instrumented by the Central Muon Upgrade (CMP), located after $\sim 8~\lambda_I$. The central muon extension (CMX), which covers the pseudorapidity range $0.6 < |\eta| < 1.0$, provides muon identification over 67% of the azimuth and is located behind $\sim 6~\lambda_I$. The dimuon trigger used for this analysis is described in Reference [2].

Muons for reconstruction of $J/\psi$ candidates are selected using the following criteria: 1) The difference in the distance in the transverse plane between the track in the muon chamber and the extrapolated CTC track is required to be less than $3\sigma$, where $\sigma$ is calculated using the quadratic sum of the multiple scattering and measurement uncertainties. For muons in the CMU, where the $z$ position is measured, the $3\sigma$ matching requirement is also made in the longitudinal view. 2) The energy deposited in the hadronic calorimeter by each muon is required to be greater than 0.1 GeV, indicating the presence of a track. 3) The reconstructed $p_T$ of at least one of the muon tracks is required to be $> 2.5$ GeV/c.

To insure that the decay point of the $B$ meson is well measured, the following quality cuts are applied: 1) each track must contain at least 2 CTC axial superlayers each of which must have at least 5 hit layers; 2) each track must contain at least 2 CTC stereo superlayers each of which must have at least 2 hit layers; 3) both muons must be reconstructed in the SVX.

The invariant mass for oppositely charged dimuon candidates obtained with these cuts has been calculated after constraining the two tracks to come from a common point in space ("vertex constraint"). The total number of events in the signal region (defined as $\pm 80$ MeV/c$^2$ from the world average value of the $J/\psi$ mass [9]) is 58338. The number of $J/\psi$ candidates after background subtraction is $49630 \pm 260$.

Using this $J/\psi$ sample, we have searched for the decay $\psi(2S) \to J/\psi \pi^+ \pi^-$. To improve the mass resolution, the four tracks are vertex constrained and the dimuon mass is simultaneously constrained to the world average $J/\psi$ mass. Combinations where the fit $\chi^2$ corresponds to a confidence level of less than 1% are rejected. Within a mass window of $\pm 20$ MeV/c$^2$ of the world average $\psi(2S)$ mass [9], we obtain a total of $764 \pm 53$ events after background subtraction.

$K_S^0$ candidates are selected by requiring two oppositely charged tracks with impact parameters with respect to the primary vertex of at least $2\sigma$, where $\sigma$ is the quadratic sum of the measurement error on the impact parameter and

the size of the beam spot. The $K^0_S$ candidate is required to have a positive decay length with respect to the $J/\psi$ vertex, and its impact parameter (computed as the minimum distance in the transverse plane between the $K^0_S$ flight path and the $J/\psi$ vertex) is required to be less than 2 mm. Combinations with a mass more than 20 MeV/c$^2$ from the world average $K^0_S$ mass [9] are rejected.

$B$ candidates are reconstructed by combining a $\Psi$ candidate either with a track (assumed to be a $K^+$), or with a $K^0_S$ candidate plus a track (assumed to be a $\pi^+$) forming a $K^*(892)^+$ candidate, or with a $K^0_S$ candidate, or with two oppositely charged tracks (assumed to be a $K^+$ and a $\pi^-$) forming a $K^*(892)^0$ candidate. The $J/\psi$ and $\psi(2S)$ candidates are mass constrained and all tracks (except $K^0_S$ decay products) are constrained to come from a single vertex. $K^0_S$ decay products are mass and vertex constrained and the $K^0_S$ is constrained to point to the $B$ decay vertex. Combinations where the $K^*(892)$ mass is more than 80 MeV/c$^2$ from the world average mass [9] are rejected. In all cases, the fit is required to have a $\chi^2$ which corresponds to a confidence level of better than 1%.

Cuts on the $B$ meson and K $p_T$ are optimized to give the smallest statistical uncertainty on the number of $B$ mesons after background subtraction. A Monte Carlo simulation is used to model the signal coming from $B$ meson decays, while data in the sidebands of the invariant mass distributions are used to determine the number of background events. The $p_T$ cuts obtained by this proceedure are not strongly decay-mode dependent. We therefore use the same selection criteria for all channels: $p_T(B) > 6.0$ GeV/c and $p_T(\text{K}) > 1.25$ GeV/c.

The reconstruction is applied to all possible track combinations, allowing the same $J/\psi$ to be used for more than one $B$ candidate. Since such duplicate events could bias the lifetime measurement, we choose only one candidate per event in a $\pm 120$ MeV/c$^2$ window around the world average $B$ mass [9]. First, for duplicate candidates arising from the ambiguity of the mass assigned to the two tracks forming the $K^*(892)^0$, only the candidate with the $K\pi$ or $\pi K$ mass assignment closest to the world average $K^*(892)^0$ mass is kept; this choice decreases the number of $B^0$ candidates by $\sim 30\%$. Then, among the remaining candidates in the mass window, we choose the one with the highest confidence level returned by the fit described above.

The upper plots in Figure 1 show the invariant mass distributions of all $B^+$ and $B^0$ candidates. Background in these distributions comes from combinations of $J/\psi$'s with tracks produced during the $b$-quark fragmentation or with other remnants of the $p\bar{p}$ collision. These tracks should reconstruct to the primary vertex. Thus the background is largest for events where the decay distance is small. This fact is demonstrated in the lower plots of Figure 1.

We define the $B$ signal region of the invariant mass distribution to be the region within $\pm 30$ MeV/c$^2$ of the world average $B$ mass. Sideband regions, used to determine the shape of the background under the mass peak, are defined

6

to have invariant mass between 60 and 120 MeV/c$^2$ from the world average $B$ mass. These sidebands have been chosen to exclude the regions where $B \to \Psi K \pi$ events are kinematically allowed.

The technique used to measure the $B^+$ and $B^0$ lifetimes is similar to the one used by CDF to measure the average $B$ lifetime [2]. For each $B$ candidate, the two dimensional decay distance $L_{xy}$ is calculated as the projection of the vector $\vec{X}$ pointing from the primary to the secondary vertex onto the transverse momentum of the $B$ candidate. Since the momentum of the $B$ meson is known, the proper decay length $c\tau$ can be determined:

$$c\tau = L_{xy} \frac{M_B}{|\vec{p}_T^B|} = \vec{X} \cdot \hat{p}_T^B \frac{M_B}{|\vec{p}_T^B|}.$$

The primary vertex position is approximated by the mean beam position, determined run-by-run using SVX information and averaging over many events. We choose not to measure the primary vertex event-by-event because the presence of a second $b$ quark coupled with the low multiplicity in the $J/\psi$ events can lead to a systematic bias in the lifetime. This technique would not improve the statistical uncertainty of the measurement significantly.

The lifetimes of the $B^+$ and $B^0$ are obtained by performing separate unbinned maximum likelihood fits to the $c\tau$ distributions of the charged and neutral event samples. For each sample, the fit is made simultaneously to the signal and sideband distributions. The number of background events in the peak region is constrained to be equal, within Poisson fluctuations, to the number of events in the normalised sideband distribution. The fits, which are shown in Figure 2 and summarized in Table I, are performed under the following assumptions:

- The signal region contains both signal and background events. The proper decay lengths of the signal events are distributed according to an exponential function convoluted with a Gaussian resolution function. The slope of the exponential ($\lambda$) is the proper decay length to be measured. The Gaussian resolution for each event is the measurement error on $c\tau$. The fit parameter $\alpha$ gives the fraction of signal events in the peak region while $\mathcal{N}$ gives the number of signal events.

- Background events in the signal region are assumed to have the same $c\tau$ distribution as the events in the sideband region. The proper decay lengths of the background events are distributed according to the sum of a Gaussian resolution function and two exponential tails, where the exponentials are used to model the positive and negative lifetime tails [2]. The fit parameters $f^+$ and $f^-$ are the fraction of background events in the positive-side and negative-side exponentials, while $\lambda^+$ and $\lambda^-$ are the exponential slopes.

Estimates of the systematic uncertainties on the lifetime measurements are listed in Table II. The uncertainties

7

due to residual misalignment, trigger bias, and movement of the beam-spot within a single run are determined in the same manner as Reference [2] and are completely correlated in the $B^+$ and $B^0$ lifetime measurements. The result of the maximum likelihood fit depends on the decay-length error calculated for each event. We have varied these errors by a common scale factor which is allowed to float in the fit; this variation changes the proper decay length by $\leq 2$ $\mu$m. The effect of non-gaussian tails in the resolution function has been studied by including exponential tails in the fit and allowing both the slope and normalization of these tails to vary freely. This study yields a 7 $\mu$m (4 $\mu$m) uncertainty in the proper decay length of the $B^+$ ($B^0$). From studies using event samples generated with a Monte Carlo technique, we determine that the fitting procedure biases the lifetime measurements by $\leq 2$ $\mu$m.

An additional source of uncertainty on this measurement comes from the modeling of the background $c\tau$ distribution. Although the confidence levels of the fits are adequate (Table I), we estimate the systematic uncertainty associated with the choice of parameterization by comparing the fitted lifetime to that obtained if an extreme model of the background shape is used. We add to the background parameterization a flat component in the range $0 < c\tau < 0.2$ cm. The normalization of this flat component is allowed to vary in the fit. Based on this study, we assign a systematic uncertainty of 6 $\mu$m (21 $\mu$m) to the $B^+$ ($B^0$) proper decay length due to uncertainties in the shape of the background distribution.

Combining the above sources of uncertainty in quadrature, we estimate a systematic uncertainty of 16 $\mu$m (25 $\mu$m) on the $B^+$ ($B^0$) mean decay length. When calculating the uncertainty on the lifetime ratio, we remove the correlated systematic uncertainties indicated above. The final results are:

$$\tau^+ \quad = \quad 1.61 \pm 0.16 \text{ (stat)} \pm 0.05 \text{ (sys) ps}$$
$$\tau^0 \quad = \quad 1.57 \pm 0.18 \text{ (stat)} \pm 0.08 \text{ (sys) ps}$$
$$\tau^+/\tau^0 \quad = \quad 1.02 \pm 0.16 \text{ (stat)} \pm 0.05 \text{ (sys)}$$

These measurements are consistent with those presented in References [5] and [6], but have a smaller uncertainty. They are also consistent with recent measurements of the average $b$-hadron lifetime ($1.49 \pm 0.038$ ps) [11].

The measurement of $\tau^0$ can be combined with CLEO measurements of the $q^2$ dependence of the partial width for $B^0 \to D^{*-}\ell^+\nu_\ell$ to extract a value of $|V_{cb}|$ [10]. Using the method and results of Reference [12] and the value of $\tau^0$ quoted here, we find $|V_{cb}| = (36 \pm 5 \pm 4) \times 10^{-3}$. Using our measurement of $\tau^0$, there is no increase in the overall error on $|V_{cb}|$ and any systematic uncertainty associated with using the inclusive lifetime is eliminated.

We thank the CDF technical support staff at all CDF institutions for their hard work and dedication. We also

| Parameter | | $B^+$ | | | $B^0$ | | |
|---|---|---|---|---|---|---|---|
| $\lambda$ | [$\mu$m] | 482 | $\pm$ | 48 | 472 | $\pm$ | 55 |
| $\alpha$ | [%] | 26.9 | $\pm$ | 2.3 | 14.4 | $\pm$ | 1.8 |
| $\mathcal{N}$ | [events] | 148 | $\pm$ | 16 | 121 | $\pm$ | 16 |
| $f^-$ | [%] | 2.3 | $\pm$ | 0.6 | 1.3 | $\pm$ | 0.3 |
| $\lambda^-$ | [$\mu$m] | 349 | $\pm$ | 79 | 514 | $\pm$ | 114 |
| $f^+$ | [%] | 10.2 | $\pm$ | 1.4 | 11.0 | $\pm$ | 1.2 |
| $\lambda^+$ | [$\mu$m] | 281 | $\pm$ | 37 | 191 | $\pm$ | 19 |
| Confidence level | | 43% | | | 32% | | |

TABLE I. Results of lifetime fits.

| Source of systematic error | Error on $B^+$ | Error on $B^0$ |
|---|---|---|
| Residual misalignment | 10 $\mu$m | 10 $\mu$m |
| Trigger bias | 6 $\mu$m | 6 $\mu$m |
| Beam stability | 5 $\mu$m | 5 $\mu$m |
| Scale factor for resolution | 1 $\mu$m | 2 $\mu$m |
| Non-gaussian tails in resolution function | 7 $\mu$m | 4 $\mu$m |
| Fitting procedure bias | 2 $\mu$m | 2 $\mu$m |
| Background parametrisation | 6 $\mu$m | 21 $\mu$m |
| Total | 16 $\mu$m | 25 $\mu$m |

TABLE II. Summary of systematic uncertainties

$^{(a)}$ Visitor.

[1] P. Abreu *et al.* Z. Phys. C **53** 567 (1992); B. Adeva *et al.* Phys. Lett B **270** 111 (1992); O. Adriani *et al.* Phys. Lett. B **317** (1993) 474; P.D. Acton *et al.* Phys. Lett. B **274** 513 (1992); D. Buskulic *et al.* Phys. Lett. B **295** (1992) 174; D. Buskulic *et al.* Phys. Lett. B **314** (1993) 459; P.D. Acton *et al.* CERN-PPE/93-92, submitted to Z. Phys. C.

[2] F. Abe *et al.* Phys. Rev. Lett. **71** 3421 (1993).

[3] D. Besson, *Recent Bottom Physics Results from Threshold Machines*, to be published in the Proceedings of the 1993 Lepton-Photon Conference, August 1993, Ithaca, New York.

[4] M.B. Voloshin and M.A. Shifman, Sov. Phys. JETP **64** 698 (1986); G. Altarelli and S. Petrarca, Phys. Lett. B **261** 303 (1991); I. Bigi and N. Uraltsev, Phys. Lett. B **280** 271 (1992).

[5] S. Wagner *et al.* Phys. Rev. Lett. **64** 1095 (1990); P. Abreu *et al.* Z. Phys. C **57** 181 (1993); D. Buskulic *et al.* Phys. Lett. B **297** 449 (1992); D. Buskulic *et al.* Phys. Lett. B **307** 194 (1993); D. Buskulic *et al.* Phys. Lett. B **314** 459 (1993); P.D. Acton *et al.* Phys. Lett. B **307** 247 (1993).

[6] H. Albrecht *et al.* Phys. Lett. B **275** 195 (1992); R. Fulton *et al.* Phys. Rev. D **43** 236 (1991); M. Artuso *et al.* *A Measurement of the Charged and Neutral B Meson Lifetime Ratio*, contributed paper to the 1993 Lepton-Photon Conference, August 1993, Ithaca, New York.

[7] F. Abe *et al.* Nucl. Inst. and Meth. A271 387 (1988) and references therein.

[8] D. Amidei *et al.* FERMILAB PUB-94/024/E, to be published in Nucl. Inst. and Meth.; B. Barnett *et al.* Nucl. Inst. and Meth. A **315** 125 (1992); O. Schneider *et al.* Proceedings of the 7$^{th}$ Meeting of the American Physical Society, Division of Particles and Fields, Fermilab, Nov 1992, World Scientific Press, 1743.

[9] Particle Data Group, K. Hikasa *et al.* Phys. Rev D45 (1992).

[10] M. Neubert, Phys. Lett. B **264** 455 (1991).

[11] W. Venus, *Recent Results on Bottom Physics above Threshold*, to be published in the proceedings of the 1993 Lepton-Photon

[12] G. Crawford *et al.* CLEO CONF 93-30, *A Measurement of BR($\overline{B}^0 \rightarrow D^{*+}l^-\overline{\nu}$)*, contributed paper to the 1993 Lepton-Photon Conference, August, 1993, Ithaca, New York.
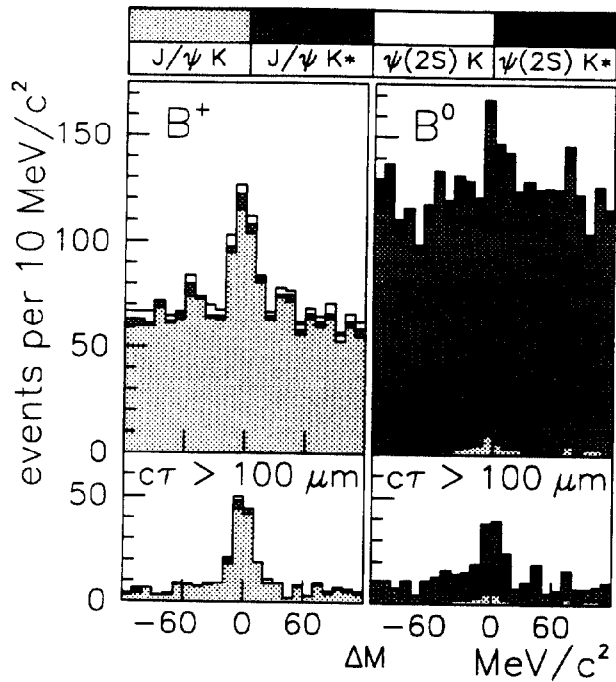
FIG. 1. The invariant mass distribution for all reconstructed $B^+$ and $B^0$ mesons. $\Delta M$ is the measured mass minus the world average $B$-meson mass. The upper plots show all events passing the selection described in the text. The lower plots show the subset of events with the proper decay length $c\tau > 100$ $\mu$m. In the fit to the lifetime, the peak region is defined as the 6 central bins and the sideband regions are defined as the 6 leftmost and the 6 rightmost bins.
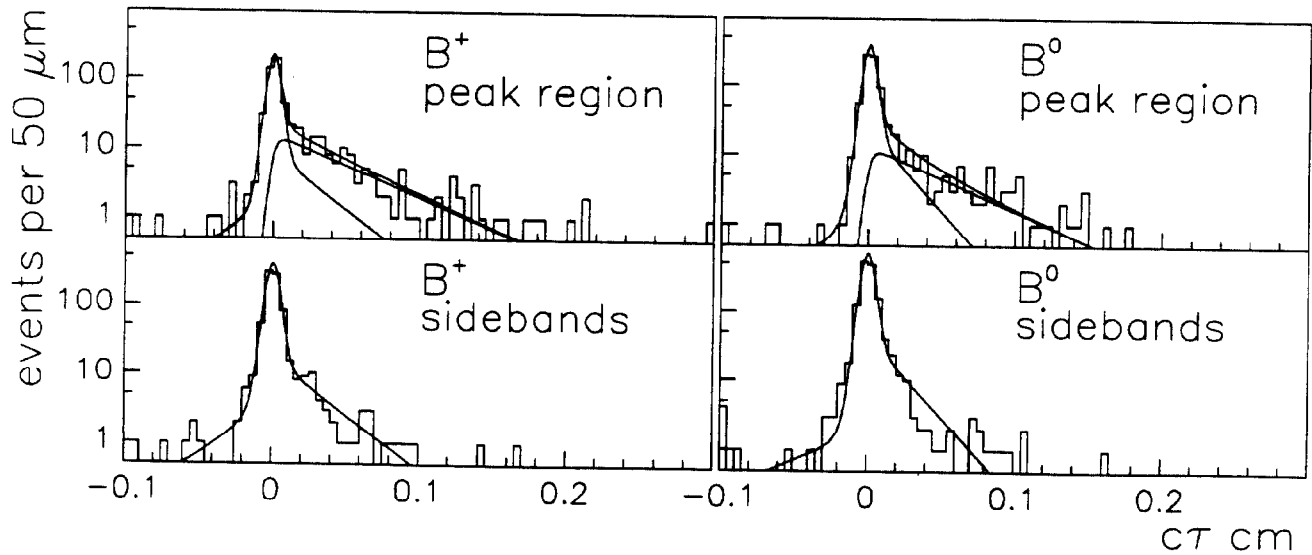
FIG. 2. The $c\tau$ distributions of all reconstructed $B^+$ and $B^0$ mesons. The upper (lower) histograms show the peak (sideband) region distributions. The first (last) bin of each histogram shows the number of underflow (overflow) events. The superimposed curves are the contributions from the signal, the background and their sum, as determined from the likelihood fit described in the text.